

# Improvement of Wear Resistance of AZ31 B Mg Alloy by Applying Oxide-SiC Nanocomposite Coating via Plasma Electrolytic Oxidation

Reza Ebrahimi-kahrizsangi, Hadi Vasiri Vatan

Advanced Materials Research Center, Materials Engineering Department, Najafabad Branch, Islamic Azad University, Najafabad, Isfahan, Iran  
rezaebrahimi@iaun.ac.ir, hadi\_nasiri\_vatan@yahoo.com

**Abstract** – Ceramic coatings were produced on the surface of AZ31 B Mg alloy using a plasma electrolytic oxidation (PEO) process from an aluminate-silicate electrolyte containing SiC nanoparticles at different coating times. Scanning electron microscopy equipped with energy dispersive x-ray spectroscopy was employed to monitor morphological and chemical changes of obtained oxide coatings. It was found that in presence of SiC nanoparticles, porosity as well as mean diameter of pores decreased. Meanwhile, the mean diameter of pores increased with prolonging coating time. The wear tests were conducted using a pin-on-disk tribometer under normal load of 5 N for 1500 cm. The wear results showed that the wear rate of ceramic-SiC nanocomposite coatings was less than ceramic ones. The higher hardness of ceramic-SiC nanocomposite coatings could be the main reason of decrease in wear of these coatings in comparison with simple coatings.

**Keywords:** Ceramic coating, Mg alloy, plasma electrolytic oxidation, SiC nanoparticles, wear resistance

## 1. Introduction

In recent decades, the demand for light metals due to increasing pollution weather and fuel cost is growing in many industry applications such as aerospace and automobile [1]. Magnesium and its alloys because of their unique properties such as low density, high specific strength and stiffness have been extensively used for such applications [2]. Nevertheless, a poor resistance can restrict their wide usage [3, 4]. Various types of protective coatings namely physical vapour deposition, chemical vapour deposition, electrodeposition and plasma electrolytic oxidation (PEO) have been suggested for improvement of magnesium and its alloys [5-7]. Among these, the PEO is a simple, environmental friendly and promising electrochemical approach that can produce ceramic coating [8]. The composition and structural of coating can be controlled by the electrolyte composition and concentration. The PEO coating on Mg alloys are applied from electrolytes containing phosphate, silicate and aluminate, and the formed coatings are generally composed of MgO-Mg<sub>3</sub>(PO<sub>4</sub>)<sub>2</sub>, MgO-Mg<sub>2</sub>SiO<sub>4</sub> and MgO-MgAl<sub>2</sub>O<sub>4</sub>, respectively [9]. However, a surface porosity of PEO coating leads to decrease of their performance. Recently, most studies have focused on improving the corrosion behaviour of PEO coatings containing particles such as TiO<sub>2</sub>, ZrO<sub>2</sub>, CeO<sub>2</sub>, Al<sub>2</sub>O<sub>3</sub> [10-12].

Silicon carbide particles have been used as reinforcement phase for increment of wear and corrosion resistance of nickel matrix coating produced by electrodeposition [13, 14]. However, tribological behaviour of PEO coating reinforced with SiC nanoparticles has been rarely studied. Hence, to explore the potential benefit of SiC nanoparticles in PEO coatings on Mg alloys, this present research investigated the tribological performance of PEO coatings applied on an AZ31B Mg alloy in the electrolytes containing SiC nanoparticles with different coating time.

## 2. Experimental procedure

The substrate material used for the present investigation was AZ31 B magnesium alloy with dimensions of 2 cm × 2 cm × 1 cm. Prior to PEO treatment, the samples were mechanically ground with silicon carbide emery papers (up to 1000 grit); rinsed with water, then degreased in ethanol and finally dried with hot air. The treatment device for plasma electrolytic oxidation process consists of a high power supply unit, a stirring and cooling system, the AZ31 B Mg alloy substrate and a stainless steel cylinder container which acts as anode and cathode, respectively. The electrolytic solution was composed of an aqueous solution of NaAlO<sub>2</sub> (2 g/L), Na<sub>2</sub>SiO<sub>3</sub> (2 g/L) and KOH (1.5 g/L) without and with SiC nanoparticles (5 g/L). The size of SiC nanoparticles used in this study was less than 80nm, as shown in Fig. 1. To prevent the agglomeration of Al

particles, the electrolytes containing different amounts of SiC nanoparticles were premixed and stirred by a magnetic stirrer for 12 h and then by ultrasonic agitation for 30 min just prior to PEO process. The temperature of the electrolytes during the treatment was constantly maintained at  $20 \pm 2$  °C by a water cooling system, and the electrolyte was stirred continuously during the treatment. The PEO coating was prepared in this solution at a current density of  $11.5 \text{ A/cm}^2$  for different oxidation time (5 and 20 min). The processed PEO coatings without and with SiC nanoparticles for coating times of 5 and 20 min are referred to as P5, P20, SiC5 and SiC20, respectively.

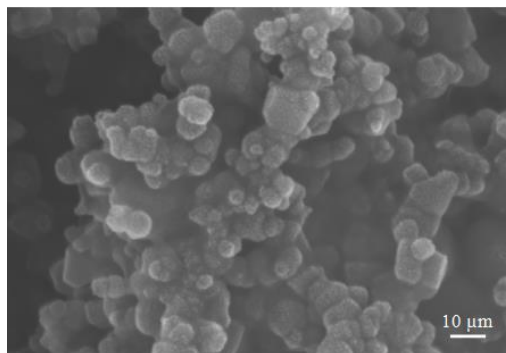


Fig. 1: SEM image of the SiC nanoparticles.

The surface morphology and elemental analysis of the samples were studied using a VegaTescan scanning electron microscope (SEM) equipped with energy dispersive X-ray spectrometer (EDS). The hardness of the coatings was measured using HXD-1000 microhardness tester with Vickers indenter, employing a load of 25 g for 10 s.

The wear tests were performed on a pin on-disk tribometer using the Mg disk coated PEO. The tungsten carbide (WC–6 wt.% Co) pins was used as slider. The diameter of the pins was 8 mm with 5 mm radius on their tips. The wear tests were performed under a normal load of 5 N at a constant sliding speed of 0.05 m/s for a sliding distance of 1500 cm at wear testing temperatures of 25 °C in dry conditions. Prior to each test, all contact surfaces were ultrasonically cleaned in acetone, dried and weighed to a precision of 0.1 mg. Three wear tests were carried out for each condition and the average weight loss was calculated. The coefficient of friction was calculated using the measured friction and the normal load.

## 2. Results and Discussion

Surface morphologies of the coatings produced in the electrolyte containing 0 and 5 g/L SiC under different processing times are shown in Fig.2. The appearance of pores on the surface of the coating is characteristic of PEO coatings. A comparative evaluation of the coatings indicates that the size of pores in PEO coatings obtained from the SiC free electrolyte is larger than that obtained from the electrolyte containing suspended SiC nanoparticles. It was reported that the trapped nanoparticles inside the pores led to close of the pores outfalls, and consequently, a decrease in surface porosity and pores diameter of nanocomposite coatings. Moreover, as shown this figure, the surface pore size increased with increasing the coating time. This trend was also observed by Bayati et al. [15, 16]. They showed that when a structural defect such as pore forms by an electrical discharge, it is a more susceptible place for next electron avalanches because of its lower breakdown voltage in comparison with other areas of the surface which are not porous [17].

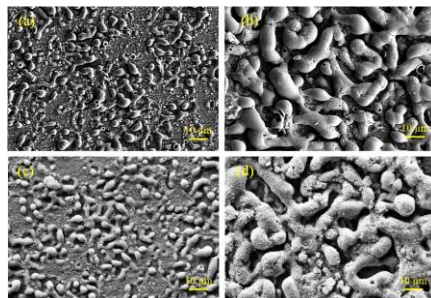


Fig. 2: SEM images of surface coatings: a)P5, b)P20, c)SiC5, d)SiC20.

To study of coatings with more details, SEM images from cross section of coatings are presented in Fig. 3. The mean thickness of coatings obtained from Fig. 3 is listed in table 1. It is observed that mean thickness of coatings increased with increasing the coating time, as expected. Furthermore, the mean thickness of nanocomposite coatings is less than simple ones. It seems that incorporation of SiC nanoparticles into oxide coatings lead to an increase in coating compactness. This finding is good agreement with other results [18].

Table 1: The mean thickness of coatings.

Sample	P5	P20	SiC5	SiC20
Mean thickness ( $\mu\text{m}$ )	3.01	7.32	2.73	4.05

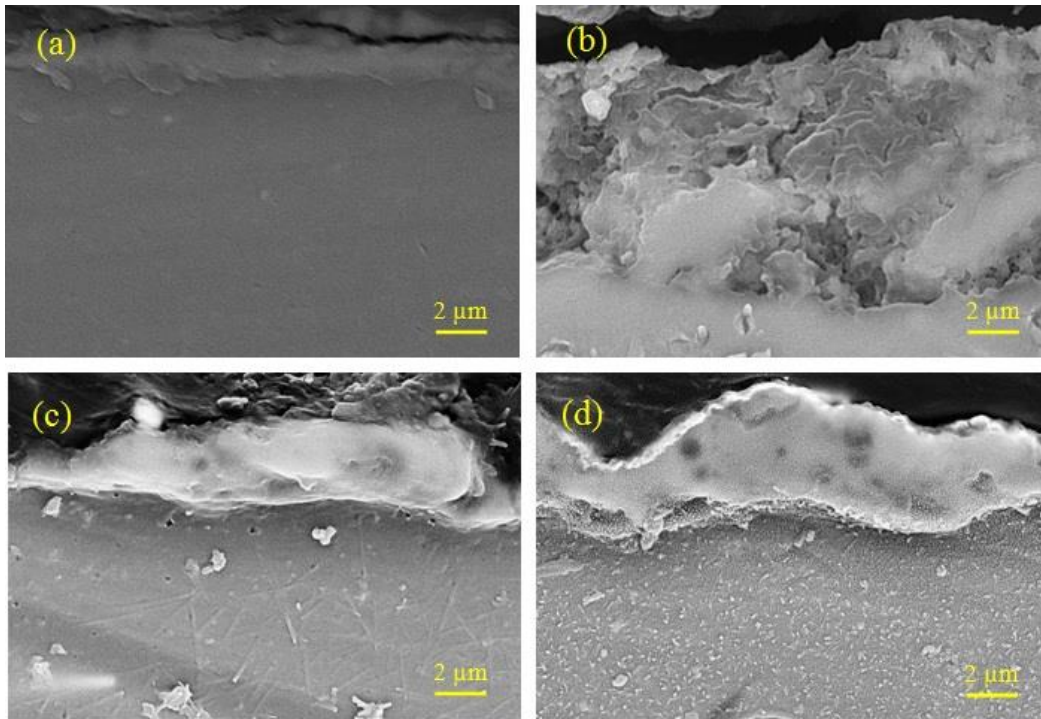


Fig. 3: SEM micrographs of cross-section of coatings: a)P5, b)P20, c)SiC5, d)SiC20.

Figure 4 presents the element distribution across the thickness of SiC20 coating, and as it can be clearly observed that all elements, including Si, are uniformly distributed across the coating.

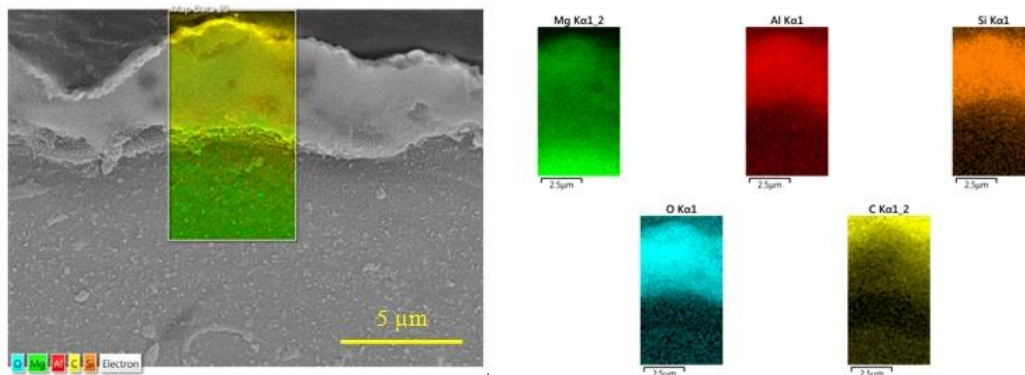


Fig. 4: EDS maps illustrating distribution of considered elements in cross section of coating SiC20.

The wear rates and hardness of the coatings under load of 5 N is shown in table 2. The wear rate of nanocomposite coatings was less than simple ones. This matter can be explained by Archard's wear equation [19]. According to the equation, the wear of material is decreased as the hardness is increased. Since the hardness of nanocomposite coatings were higher than simple ones, therefore, wear resistance of nanocomposite coatings was better than simple ones.

Table 2: The hardness and wear rate of coatings.

Sample	P5	P20	SiC5	SiC20
Hardness(HV)	91	145	174	325
Wear rate (mg/m)	0.004	0.005	0.0006	0.0004

Coefficient of friction is an important parameter during wear processes, which could be helpful in study of wear behavior of samples. Variations of coefficient of friction with sliding distance under normal load of 5 N are shown in Fig. 5. As seen in this figure, an instability in coefficient of friction of SiC20 coating is higher than P20 one. It was probably due to the low surface porosity of SiC20 coating in comparison with P20 coating.

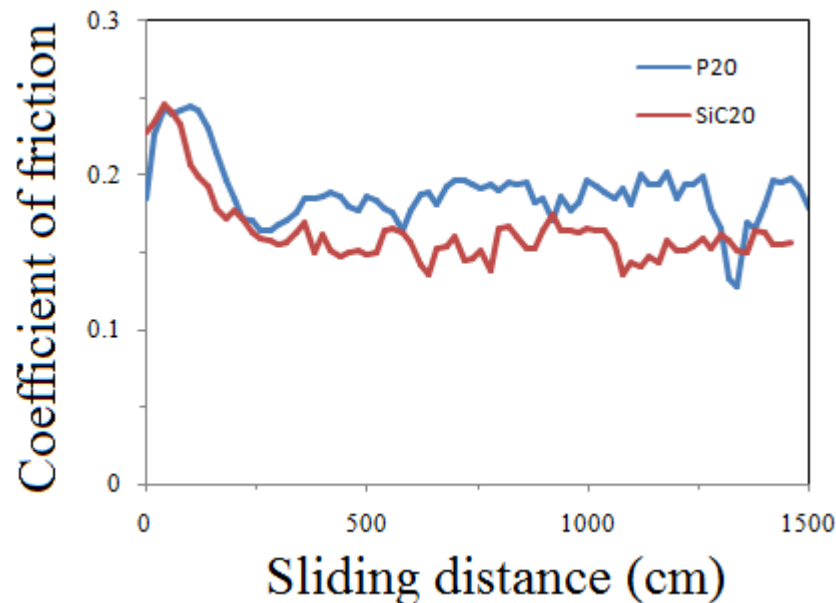


Fig. 5: Variations of coefficient of friction during sliding the pin on surface of coatings.

#### 4. Conclusion

Experiments were conducted to identify the effect of incorporation of SiC particles into oxide coating and coating time on composition, microhardness and wear resistance of coatings. It can be concluded that:

- The size of surface porosity increased with increasing the coating time. Meanwhile, surface porosity size of nanocomposite coatings was less than simple ones.
- The hardness of nanocomposite coatings was higher than simple ones.
- The wear resistance of nanocomposite coatings was better than simple ones.

#### References

- [1] J. Gray and B. Luan, "Protective coatings on magnesium and its alloys—a critical review," *J.Alloy. Compod.*, vol. 336, pp. 88-113, 2002.
- [2] H.-X. Guo, M. Ying, J.-s. Wang, Y.-S. Wang, H.-R. Dong, and H. Yuan, "Corrosion behavior of micro-arc oxidation coating on AZ91D magnesium alloy in NaCl solutions with different concentrations," *T. Nonferr. Metal. Soc China.*, vol. 22, pp. 1786-1793, 2012.

- [3] N. Yamauchi, K. Demizu, N. Ueda, N. Cuong, T. Sone, and Y. Hirose, "Friction and wear of DLC films on magnesium alloy," *Surf. Coat. Technol.*, vol. 193, pp. 277-282, 2005.
- [4] S. Yu and Z. Huang, "Dry Sliding Wear Behavior of Fly Ash Cenosphere/AZ91D Mg Alloy Composites," *J. Mater. Eng. Perform.*, vol. 23, pp. 3480-3488, 2014.
- [5] M. H. Fini and A. Amadeh, "Improvement of wear and corrosion resistance of AZ91 magnesium alloy by applying Ni-SiC nanocomposite coating via pulse electrodeposition," *T. Nonferr. Metal. Soc China*, vol. 23, pp. 2914-2922, 2013.
- [6] P. B. Srinivasan, J. Liang, C. Blawert, and W. Dietzel, "Dry sliding wear behaviour of magnesium oxide and zirconium oxide plasma electrolytic oxidation coated magnesium alloy," *Appl. Surf. Sci.*, vol. 256, pp. 3265-3273, 2010.
- [7] P. B. Srinivasan, C. Blawert, and W. Dietzel, "Dry sliding wear behaviour of plasma electrolytic oxidation coated AZ91 cast magnesium alloy," *Wear*, vol. 266, pp. 1241-1247, 2009.
- [8] A. Yerokhin, X. Nie, A. Leyland, A. Matthews, and S. Dowey, "Plasma electrolysis for surface engineering," *Surf. Coat. Technol.*, vol. 122, pp. 73-93, 1999.
- [9] H. Guo, M. An, S. Xu, and H. Huo, "Microarc oxidation of corrosion resistant ceramic coating on a magnesium alloy," *Mater. Letter.*, vol. 60, pp. 1538-1541, 2006.
- [10] L. Feng, D.-Y. Shan, Y.-W. Song, and E.-H. Han, "Formation process of composite plasma electrolytic oxidation coating containing zirconium oxides on AM50 magnesium alloy," *T. Nonferr. Metal. Soc China*, vol. 21, pp. 943-948, 2011.
- [11] T. S. Lim, H. S. Ryu, and S.-H. Hong, "Electrochemical corrosion properties of CeO<sub>2</sub>-containing coatings on AZ31 magnesium alloys prepared by plasma electrolytic oxidation," *Corros. Sci.*, vol. 62, pp. 104-111, 2012.
- [12] A. Madhankumar, E. Thangavel, S. Ramakrishna, I. Obot, H. C. Jung, K. S. Shin, *et al.*, "Multi-functional ceramic hybrid coatings on biodegradable AZ31 Mg implants: electrochemical, tribological and quantum chemical aspects for orthopaedic applications," *RSC Adv.*, vol. 4, pp. 24272-24285, 2014.
- [13] S. L. Baghal, M. H. Sohi, and A. Amadeh, "A functionally gradient nano-Ni-Co/SiC composite coating on aluminum and its tribological properties," *Surf. Coat. Technol.*, vol. 206, pp. 4032-4039, 2012.
- [14] A. Amadeh, A. Rahimi, B. Farshchian, and H. Moradi, "Corrosion Behavior of Pulse Electrodeposited Nanostructure Ni-SiC Composite Coatings," *J. nanosci. nanotechnol.*, vol. 10, pp. 5383-5388, 2010.
- [15] M. Bayati, F. Golestani-Fard, and A. Moshfegh, "How photocatalytic activity of the MAO-grown TiO<sub>2</sub> nano/microporous films is influenced by growth parameters?," *Appl. Surf. Sci.*, vol. 256, pp. 4253-4259, 2010.
- [16] F. Samanipour, M. Bayati, F. Golestani-Fard, H. Zargar, T. Troczynski, and A. Mirhabibi, "An innovative technique to simply fabricate ZrO<sub>2</sub>-HA-TiO<sub>2</sub> nanostructured layers," *Coll. Surf. B: Biointerf.*, vol. 86, pp. 14-20, 2011.
- [17] A. Rapacz-Kmita, A. Ślósarczyk, and Z. Paszkiewicz, "Mechanical properties of HAp-ZrO<sub>2</sub> composites," *J. Eur. Cer. Soc.*, vol. 26, pp. 1481-1488, 2006.
- [18] V. Rudnev, M. Vasilyeva, N. Kondrikov, and L. Tyrina, "Plasma-electrolytic formation, composition and catalytic activity of manganese oxide containing structures on titanium," *Appl. Surf. Sci.*, vol. 252, pp. 1211-1220, 2005.
- [19] J. Archard, "Contact and rubbing of flat surfaces," *J. appl. phys.*, vol. 24, pp. 981-988, 1953.